Available online at www.sciencedirect.com
SCIENCE DIRECT
Polymer 45 (2004) 8893–8900
polymer
www.elsevier.com/locate/polymer

Isothermal crystallization in PCL/clay nanocomposites investigated with thermal and rheometric methods

Ernesto Di Maio[a,*], Salvatore Iannace[b], Luigi Sorrentino[b], Luigi Nicolais[a]

[a]*Department of Materials and Production Engineering, University of Naples Federico II, P.le Tecchio 80, I-80125 Naples, Italy*
[b]*Institute of Composite Materials and Biomaterials (IMCB-CNR), P.le Tecchio 80, I-80125 Naples, Italy*

Received 1 July 2004; received in revised form 12 October 2004; accepted 14 October 2004
Available online 2 November 2004

Abstract

Nanocomposites based on biodegradable poly(ε-caprolactone), (PCL) and organically modified layered silicates (organoclay) were prepared by melt mixing. The isothermal crystallization of PCL/clay nanocomposites at different clay concentrations (from 0.1 to 10 wt%) were investigated by differential scanning calorimetry (DSC) and rheometry in dynamic tests. The results showed that the well dispersed organoclay platelets acted as nucleating agents in the PCL matrix, as confirmed by a remarkable reduction of the crystallization half-time, $t_{1/2}$. This effect was most pronounced at very low clay concentrations. In particular, in composites with 0.4% of clay, $t_{1/2}$ was one order of magnitude lower than the pure polymer. The heating thermograms, performed on PCL and on PCL/clay after isothermal crystallization showed a reduction of the melting temperature with the increase of the clay content, suggesting that the degree of perfection of the crystals and the degree of crystallinity were affected by the restricted mobility of the chains, which did not allow the growth of well developed lamellar crystals. The rheological measurements confirmed the effect of clay on crystallization kinetics. The evolution of G' and G'' vs. time was correlated to the clay concentration and to the development of the crystalline phase during isothermal experiments.

Keywords: Biodegradable; Nanocomposites; Crystallization

1. Introduction

Polymer nanocomposites based on nanoscale particulates of clays are receiving great interest, due to the markedly improved properties as compared to pure polymers or conventional particulate composites. The improvement of modulus, strength, barrier properties, heat resistance are achieved at the very low loading of the inorganic components (1–10%) compared to conventional filled polymers (20–40%).

Direct melt intercalation is being recognised as a promising approach because it can be performed by using a conventional polymer mixing or extrusion process. The preparation of the nanocomposites requires extensive delamination of the layered clay structure and complete dispersion of the resulting platelets throughout the polymeric matrix. This is readily achieved when using high surface energy polymers, which determine a good adhesion between the polymer and the clay phase. For some low-energy materials, such as polyethylene and polypropylene, the chemical modification of the polymeric matrix [1–4] is necessary for improving the dispersion process and the final properties of the nanocomposites. The commercial thermoplastics of interest to be hybridized with organoclay include styrenic polymers [5,6], polyolefins [7,8], nylons [9,10] and so on.

It is well known that the physical and mechanical properties of crystalline polymers depend on the morphology and the structure of the crystals and on the degree of crystallization. It has been recently found that the crystallization behavior and the crystalline morphology of nanocomposites are strongly affected by the presence of the clay particulates. Heterogeneous nucleation was observed in several polymers such as polyethylene [11], polyamide 6, [12], polyamide 6,6 [13], polyamide 12,12 [14], polypropylene [7,15] and syndiotactic polystyrene [16]. In most of

* Corresponding author. Tel.: +39 081 7682410; fax: +39 081 7682404.
E-mail address: edimaio@unina.it (E. Di Maio).

0032-3861/$ - see front matter © 2004 Elsevier Ltd. All rights reserved.
doi:10.1016/j.polymer.2004.10.037

the cases, the crystallization behavior of these materials was investigated by performing non-isothermal crystallization tests and in a restricted composition range. Fornes and Paul [17] have extensively analyzed the crystallization behavior of nylon 6 based melt processed nanocomposites, both in isothermal and non-isothermal condition with the DSC. The authors evidenced that, at very low levels of clay, the crystallization kinetics of the nanocomposites were dramatically increased, with respect to extruded polyamide while, increasing the concentration of clay beyond these levels retards the rate of crystallization, in some cases becoming slower than the extruded pure material. This behavior is commonly observed in particulate filled polymers: at low filler concentration the filler–polymer interfaces act as heterogeneous nucleating sites, hence increasing the nucleation rate and, therefore, the crystallization kinetics; at higher filler content, diffusion of polymer chains to the growing crystallites is hindered and the overall crystallization rate is reduced. In their system, the addition of clay resulted in significant changes in the Avrami constants: n showed a gradual decrease with increasing clay content, while, as discussed above, K showed a maximum at low clay content. Furthermore, a decrease of the degree of crystallinity was observed. Other authors have reported different behaviors in nanocomposites crystallization. Kim et al. [18] reported an increase of X_c with silica nanoparticle-filled PEN, Nam et al. [19] reported an increase of X_c in PLA filled with clay, while Lee et al. [20] reported a decrease of the degree of crystallinity in analogue system. Gopakumar et al. [11] observed a reduction of X_c and a reduction of n with clay content in melt compounded PE/clay nanocomposites.

Non-isothermal crystallization experiments on PCL are described in some works in the literature. Lepoittevin et al. [21] reported a decrease of X_c with clay content, while Hao et al. [22] and Jimenez et al. [23] did not observe a relevant variation of X_c with nanometric filler. Those authors used higher clay concentration with respect to the aforementioned works on polyamides and did not observe the maximum in the crystallization rates.

In the present study, the isothermal crystallization behavior of polycaprolactone/clay nanocomposites, with clay concentration ranging from 0.1 to 10 wt%, was investigated in order to allow a theoretical description of the effects of nanoclay on the crystallization phenomenon. To this aim, Avrami parameters of the isothermal crystallization kinetics were calculated as function of clay concentration at different temperatures. The analysis was extended to very low clay concentrations (0.1–0.4 wt%) since there is a lack of information in the literature on the evolution of crystalline morphology in PCL nanocomposites containing very low percentages of clay. The analysis was performed by combining two experimental techniques such as DSC and dynamic rheometry. This combination allows a more detailed characterization of the whole crystallization phenomenon [24].

2. Experimental

2.1. Materials

The PCL used was Solvay's CAPA® 6800, in the form of pellets and was kindly supplied by Solvay Interox Ltd, UK. The organoclay used in the preparation of nanocomposites was purchased from Southern Clay Products Inc, USA, under the commercial name of Cloisite® 30B and was used as received. According to the product information from the producer, this 2:1 montmorillonite (MMT) contains a quaternary ammonium ion containing methyl tallow bis-2-hydroxyethyl (MT2EtOT) as the organic modifier.

2.2. Samples preparation

A HAAKE RHEOMIX® 600 internal mixer with two counter-rotating roller rotors was used for the preparation of the PCL/organoclay nanocomposites with different compositions. The mixer is controlled by a measuring drive unit, HAAKE RHEOCORD® 9000. The processing temperature was set at 100 °C. The rotating speed of the rotor and the mixing time were fixed, respectively, at 100 rpm and 12 min. The following weight percentages of clay were used: 0.1, 0.4, 1, 2, 3.5, 5, 7 and 10. The latter samples will be referred, respectively, as PCL0.1, PCL0.4, PCL1, PCL2, PCL3.5, PCL5, PCL7 and PCL10. The same mixing procedure was used on pure PCL to compare pure material with its nanocomposites.

2.3. Characterization

Differential scanning calorimetry (DSC) analysis was carried out on a DSC2920 (TA Instruments, USA). The samples were heated from 20 to 100 °C at 10 °C/min under nitrogen atmosphere and kept at 100 °C for 5 min to eliminate the previous thermal history. They were then temperature-quenched to the crystallization temperatures (T_c = 40, 43 and 45 °C) for the isothermal experiments. The samples were then heated again to 100 °C at 10 °C/min to evaluate the melting behavior after the isothermal crystallization.

Rheological measurements were performed on an Advanced Rheometric Expansion System (TA instruments, USA). The isothermal crystallization experiments were performed in oscillatory mode, time sweep test at frequency of 1 rad/s and initial strain of 1%. Eight millimetre parallel plates were used in order to reduce the normal forces.

3. Results and discussion

The preparation and the characterization of nanocomposites based on biodegradable polycaprolactone (PCL) and organically modified layered silicates (organoclay) have been reported in a previous publication [25]. We showed

that the exfoliation of organoclay could be achieved via melt mixing process in the internal mixer and reported the effects of the type of organic modifier, organoclay contents and the processing temperature. We also discussed that the presence of organoclay into the PCL increases the crystallization temperature of PCL, during non-isothermal experiments. In this study, we investigated the crystallization behavior under isothermal conditions, in order to analyse the effect of the clay concentration on the crystallization kinetics.

3.1. Crystallization and melting behavior by DSC

The effect of the crystallization temperature (T_c) on the evolution of the relative crystallinity vs. time of the polymeric matrix (PCL) and of selected nanocomposites (PCL1, PCL3.5) are reported in Figs. 1–3. In the investigated temperature range, the crystallization kinetic of all the nanocomposites increased with the decrease of T_c. Also, the presence of nanoclay accelerated the crystallization phenomenon.

The well known theory of Avrami was used to analyse the increase of relative crystallinity, X_r, with time:

$$X_r(t) = 1 - \exp(-Kt^n), \quad (1)$$

where the values of K and n, which are considered to be diagnostic to the mechanism of crystallization, are respectively, related to the crystallization half time $t_{1/2}$ and the type of nucleation together with the geometry of the crystal growth [26,27]. Avrami constants K and n for our systems are summarized in Table 1. They were calculated by plotting $\log[-\ln(1 - X_r)]$ vs. $\log(t)$ and evaluating the slope, the Avrami exponent, n, and the intercept, the constant $\log(K)$. The linearized curves of PCL3.5 are reported in Fig. 4. All the analysed samples showed an initial linear behavior followed by a change in the curvature, suggesting that the Avrami model is not valid at the end of the crystallization process [11,15,28]. These results are also evident by the comparison between the experimental data and the Avrami predictions, reported in Figs. 1–3. In particular, the lack of agreement is more relevant at lower temperatures. For example, the sample containing only 1% w/w of clay, PCL1, (Fig. 2) showed a deviation from the model at $T_c = 40$ °C, while at higher temperatures the agreement was good. At higher clay concentration (Fig. 3), the deviation was observed in all the isothermal experiments. However, the highest deviation was again observed at the lowest temperature ($T_c = 40$ °C).

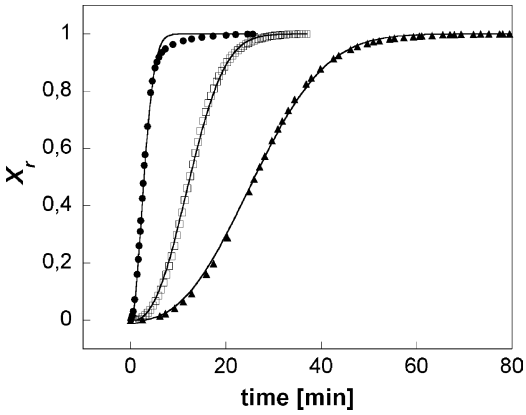

Fig. 2. Development of relative crystallinity with crystallization time during isothermal crystallization from melt of PCL1 at different test temperatures; ● 40 °C, □ 43 °C, ▲ 45 °C.

In order to analyse the effect of temperature and nanoclay concentration on this behavior, we reported, in Table 1, the critical relative crystallinity (X_{r_cr}) at which the deviation from linearity starts. A minor increase of X_{r_cr} was observed with the increase of temperature, while just 0.1 wt% of clay reduced dramatically the value of X_{r_cr}. In particular, the deviation from linearity for PCL matrix started at $X_r = 0.97$–0.99, where the crystallization phenomenon was almost complete. In case of 0.4 wt% of clay, PCL0.4, the deviation occurred at $X_r = 0.7$–0.8.

This behavior is directly related to the crystallization mechanisms that are influenced by both temperature and clay content, as confirmed by the Avrami constants n reported in Table 1. As listed in this table, this exponent,

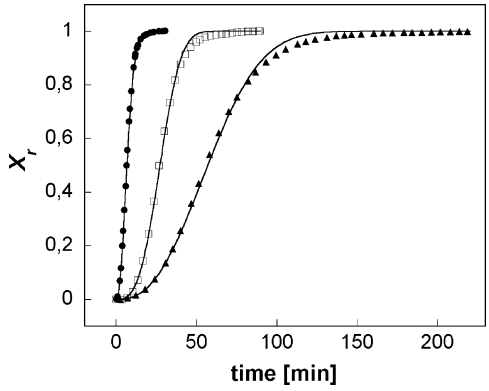

Fig. 1. Development of relative crystallinity with crystallization time during isothermal crystallization from melt of pure PCL at different test temperatures; ● 40 °C, □ 43 °C, ▲ 45 °C.

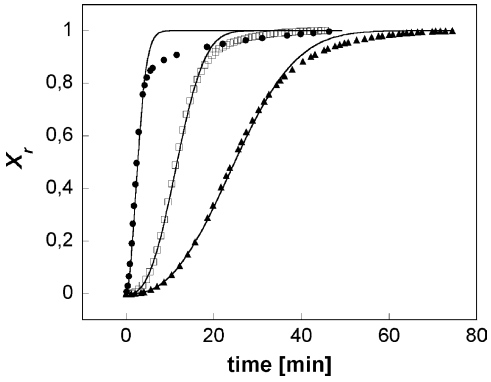

Fig. 3. Development of relative crystallinity with crystallization time during isothermal crystallization from melt of PCL3.5 at different test temperatures; ● 40 °C, □ 43 °C, ▲ 45 °C.

Table 1
Parameters from the Avrami analysis

T_c (°C)	wt% clay	n	K (min^{-n})	$t_{1/2}$ (min)	$t_{1/2\ reol}$ (min)	X_{r_cr}
40	0	2.04	1.52e-2	6.5		0.97
40	0.1	1.46	1.7e-1	2.65		0.80
40	0.4	1.43	1.04	0.7		0.80
40	1	1.93	9.37e-2	2.8		0.88
40	2	1.80	2.1e-1	2.1		
40	3.5	1.84	1.20e-1	2.45		0.83
40	7	1.89	1.55e-1	2.2		0.82
43	0	2.88	5.2e-5	26.6		0.98
43	0.1	2.41	2.7e-3	9.6		0.84
43	0.4	1.07	2.6e-1	2.5		0.70
43	1	2.57	1.05e-3	12.5		0.91
43	2	2.48	2.54e-3	9.5		
43	3.5	2.47	1.64e-3	11.5		0.91
43	5	2.28	1.90e-3	12.8		
43	7	2.34	2.10e-3	11.5		0.81
43	10	2.34	2.20e-3	11.5		
45	0	2.51	2.73e-5	56.25	70.417	0.99
45	0.1	2.44	2.8e-4	23.6	23	0.99
45	0.4	1.38	5e-2	6.5	15.5	0.72
45	1	2.55	1.71e-4	25.9	28.733	0.93
45	2	2.41	6.4e-4	22.2	30.450	
45	3.5	2.56	1.88e-4	24.0	25.833	0.91
45	7	2.57	3.3e-4	20.5	26.283	

which represents the nucleation mechanism and growth dimension, varies from a maximum of 2.9 to a minimum of 1.1. These values of the Avrami exponents indicate that crystal growth likely occurred with heterogeneous and/or athermal nucleation. The presence of nanoclay did not show a big effect on the crystallization mechanism, due to the athermal mechanism occurring in pure PCL. In particular, most of the nanocomposites crystallized at 43 and 45 °C showed an almost constant value of n ($2.4 < n < 2.9$) with the exception of the PCL0.4, for which n was much lower. The decrease of T_c (40 °C) induced a further reduction of n, with again a lower value for PCL0.4. These results suggest that n cannot be considered a temperature independent parameter.

The silicate phase acted as an efficient nucleation agent, as confirmed by the relevant increase of the kinetic constant K and by the remarkable reduction of the crystallization half-time $t_{1/2}$ (Figs. 5 and 6) [13,15]. Similar results were found in nanocomposite based on nylon 10,10 and MMT [28] and on nylon 6 and MMT [17]. As shown in Table 1, the crystallization rate was faster in presence of MMT. In particular, the addition of 0.1% of nanoclay resulted in the reduction of the crystallization half-time to less than 1/2 of that of the pure polymeric matrix. The highest crystallization rate was achieved with PCL0.4, with crystallization half time being almost one tenth of that of neat PCL. Few studies on nylon 6 have shown the same effect of the presence of the maximum in the crystallization rate

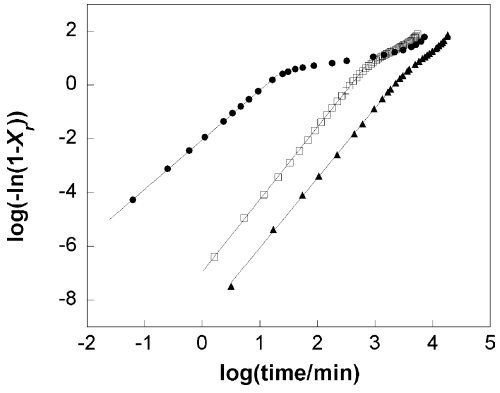

Fig. 4. Plots of $\log[-\ln(-X_r)]$ vs. $\log(t)$ for isothermal crystallization of PCL3.5 at different test temperatures; ● 40 °C, □ 43 °C, ▲ 45 °C.

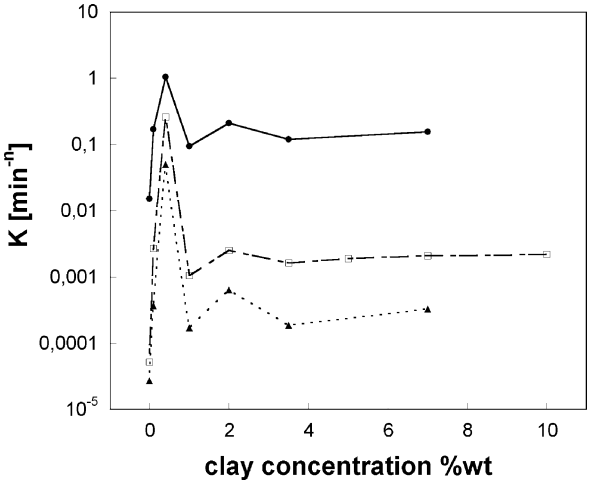

Fig. 5. Plots of Avrami constant K vs. nanoclay composition at different test temperatures; ● 40 °C, □ 43 °C, ▲ 45 °C.

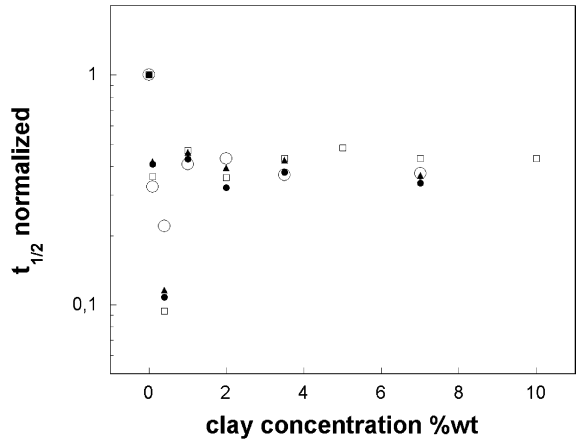

Fig. 6. Plots of normalized crystallization half time vs. nanoclay composition at different test temperatures; ● 40 °C, □ 43 °C, ▲ 45 °C, ○ rheological measurements.

occurring at additive concentration in the range 0.1–0.5 wt% [29–32].

Further increase of nanoclay content had a less remarkable effect on $t_{1/2}$. A better visualization of this behavior is given in Fig. 6, were the normalized crystallization half-times (ratio between $t_{1/2}$ of nanocomposite and $t_{1/2}$ of neat PCL, at same temperature) are reported as function of clay concentration. Here, the greatest reduction was obtained, for all T_c's, at 0.4% clay content.

The heating thermograms, performed on PCL and on selected PCL/clay after isothermal crystallization at 45 °C are reported in Fig. 7. For comparison, the heating thermogram of neat PCL, crystallized in non-isothermal conditions at −10 °C/min, is reported in the same Figure. As also reported in Table 2, all the DSC curves showed a reduction of the melting temperature with the increase of the clay content. This effect is more generally reported in the literature, on PCL nanocomposites produced with different

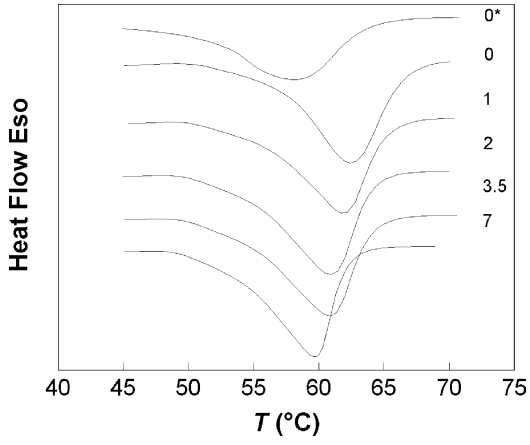

Fig. 7. DSC thermograms of PCL and of selected PCL/clay nanocomposites after isothermal crystallization at 45 °C. Number refers to clay weight concentration; 0* is the DSC thermogram of non-isothermal crystallized (−10 °C/min) pure PCL.

techniques [23] or different kind of fillers [22]. Other studies on different polymeric matrices describe different behavior. Nam et al. [19] observed an increase of T_m with clay, while Lee et al. [20] reported the opposite trend. Most of the works on nanocomposites report, anyway, a decrease of T_m with clay [13,28]. A possible explanation for this behavior is that, at the temperature investigated, the presence of the inorganic platelets greatly increases the nucleation rate, whose characteristic time is much lower than the time required for chain disentanglement. Then, the degree of perfection of the crystals and the achieved degree of crystallinity (see Table 2) were affected by the restricted mobility of the chains, which did not allowed the growth of well developed lamellar crystals [12,16]. With increasing clay content, the higher restriction of chains leaded to less perfect crystal and the melting peak shifted to lower temperature.

3.2. Crystallization behavior by rheometry

The isothermal crystallization measured with rheological tests was performed at 45 °C, where the induction time was high enough to avoid undesired premature crystallization during cooling. Fig. 8 reports the effect of clay content on the variation of G' vs. time during crystallization from the melt at 45 °C. These curves are similar to the one reported on the crystallization of Nylon 6 by Khanna [33], which first evidenced the efficacy of the rheometric technique to investigate the crystallization phenomenon. Here, again, the clay speeded up the structurization processes and the effect was maximum with PCL0.4. The crystallization half-time measured with the rheometer are reported in Table 1, while Fig. 6 reports the normalized crystallization half-time vs. clay content, showing substantial agreement of the time scales between the two experimental techniques. Moreover, G' curves slowly tend to a plateau after the crystallization, evidencing the secondary crystallization effects.

Fig. 9 reports the time evolution of G''. The increase of G'' during the crystallization of PCL and PCL nanocomposites showed a different behavior from the evolution of G' vs. time, In this case, we observed a maximum of G'' before reaching a sort of plateau. The shape of this peak is somehow dependent on the clay content. This unique behavior can also be observed in the evolution of tan δ vs. time (Fig. 10). Lin et al., instead, observed a substantial similarity between G' and G'' during crystallization of PP [34]. Here, the presence of nanoclay modifies the dissipative behavior of the composites during the growth of the crystals. For some compositions tan δ increased in the first stage of the crystallization process. For example, in nanocomposites containing 7% clay the peak is located around 15 min where the degree of crystallinity is very low (see Fig. 8). We believe that this behavior can be attributed to the interaction between the newly formed crystals on the clay surface at the early stage of crystallization that increase the dissipative capability of the nanocomposites. In other terms, depending

Table 2
DSC melting data for PCL/clay nanocompostites after isothermal crystallization

T_c (°C)	wt% clay	ΔH_c (J/g)	T_m (°C)	ΔH_m (J/g)	X_c[a]
40	0	48.29	59.40	60.02	0.42
40	0.1	47.48	58.83	63.37	0.45
40	0.4	46.13	57.5	57.50	0.41
40	1	44.15	59.55	59.33	0.42
40	2	43.31	59.07	56.58	0.41
40	3.5	42.26	59.65	56.89	0.42
40	7	41.05	58.44	52.10	0.39
43	0	55.37	59.7	62.98	0.44
43	0.1	52.45	60.57	64.61	0.46
43	0.4	45.06	59.61	61.49	0.43
43	1	50.17	60.11	60.01	0.43
43	2	47.35	59.64	60.06	0.43
43	3.5	48.32	59.74	61.20	0.45
43	5	47.39	59.64	60.10	0.45
43	7	47.92	59.86	58.62	0.44
43	10	46.44	58.73	57.33	0.45
45	0	57.09	62.43	62.39	0.44
45	0.1	51.85	61.63	66.63	0.47
45	0.4	47.66	61.63	62.18	0.44
45	1	46.77	61.72	61.72	0.44
45	2	44.88	60.95	60.24	0.43
45	3.5	45.73	60.86	59.00	0.43
45	7	45.12	59.77	56.02	0.41

[a] $\Delta H_m^0 = 142$ J/g, Wunderlich B. Macromolecular Physics, vol. 3. New York: Academic Press; 1980, p 54.

on the nucleation rate and the amount of heterogeneous nuclei that are forming on the clay surface, the relative increase of G'' compared to the increase of G' determines the shape of tan δ vs. time. The number and the size of the crystals and the number of clay platelets (exfoliated and intercalated) influence the local mobility of the amorphous chains determining the complex behavior of tan δ. A better insight into the crystallization phenomenon is shown in Fig. 11, which reports the G', G'' and tan δ for pure PCL and for PCL7. As discussed in the X-ray analysis of our previous publication [25], clay exfoliation by melt compounding PCL and Cloisite 30B becomes difficult when the clay concentration is higher than 5% wt. At these concentrations, exfoliated and intercalated clay platelets coexist in the composite, therefore, creating new possible dissipative mechanisms that contribute to this behavior, not observed in pure PCL and in lower clay concentration nanocomposites, for which clay exfoliation is reported to be extensive. Finally, Fig. 12 summarizes the rheometric test results, by reporting the final value of G', G'' and tan δ as a function of clay content. Both G' and G'' showed a maximum at 5 wt% of clay, while tan δ increases monotonically. The final value of G' is affected by the degree of crystallinity and by the

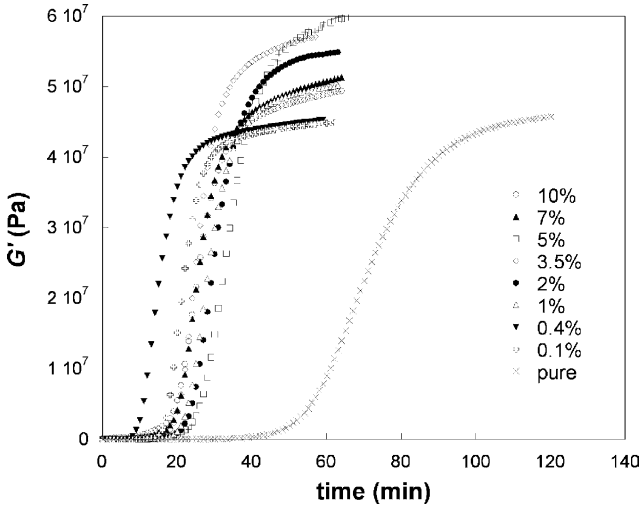

Fig. 8. G' evolution of PCL and of PCL/clay nanocomposites during isothermal crystallization at 45 °C with the rheometer.

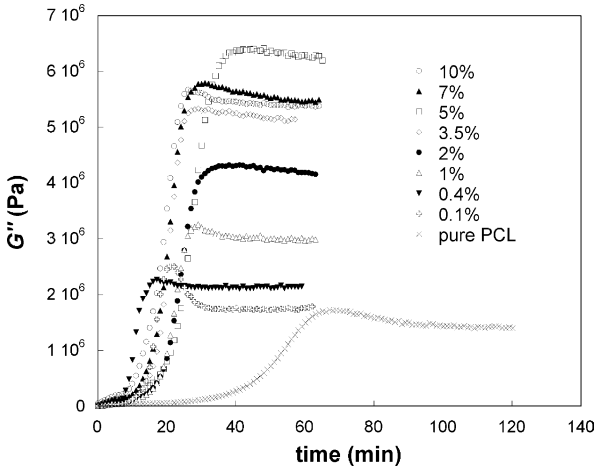

Fig. 9. G'' evolution of PCL and of PCL/clay nanocomposites during isothermal crystallization at 45 °C with the rheometer.

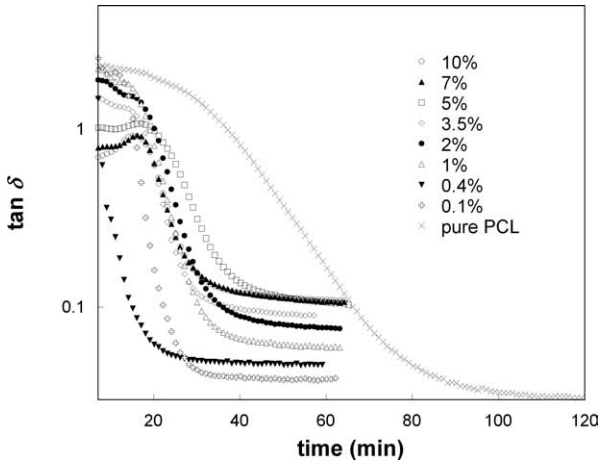

Fig. 10. Tan δ evolution of PCL and of PCL/clay nanocomposites during isothermal crystallization at 45 °C with the rheometer.

stiffening effect of clay. It is interesting to note that G' increases up to 5% of clay, despite the reduction of the crystallinity. Exfoliated clay platelets are known to increase in a more efficient way the elastic properties than intercalated ones. At concentrations higher than 5% clay contributes negligibly to the elastic properties and the reduction of G' is mainly due to the lower degree of crystallinity. Similar consideration can be depicted for G'', in which several new mechanisms, with respect to the pure polymeric matrix, contribute to the dissipative behavior. In fact, several kinds of clay/polymer interfaces provide novel dissipative processes that implicate different behavior whether: (a) the clay is exfoliated or intercalated; (b) the clay is connecting more molecules or crystals; (c) the clay is stacked to the amorphous or to the crystalline phase. Further studies need to be performed in this direction, to address the different roles of these actors of the complex scene of the viscoelastic behavior of nanocomposites. Finally, the

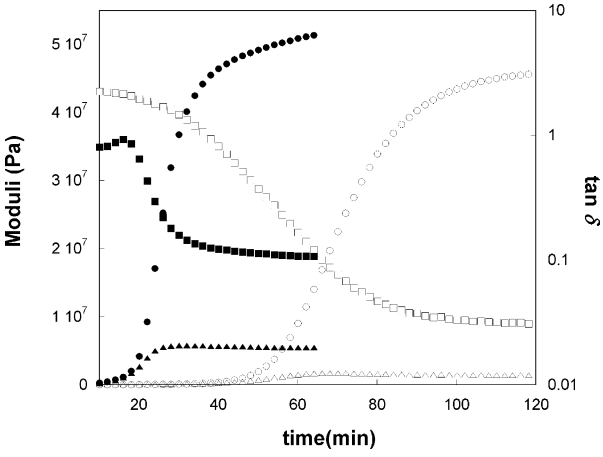

Fig. 11. G′, G″ and tan δ evolution in isothermal crystallization at 45 °C with the rheometer; open symbols, pure PCL, closed symbols, PCL7 nanocomposite; ● G′, ▲ G″, ■ tan δ.

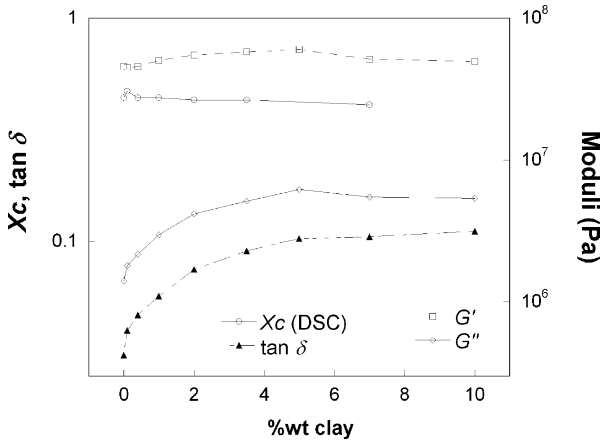

Fig. 12. Final values from rheometric tests.

measurement of the viscoelastic properties of the molten or solidified nanocomposites is a powerful tool to gain information on the degree of exfoliation of this type of hybrid materials.

4. Conclusions

The isothermal crystallization of polycaprolactone/clay nanocomposites at different clay concentrations showed that the well dispersed organoclay platelets acted as nucleating agents in PCL matrix, remarkably reducing the crystallization half-time $t_{1/2}$. This effect was maximum for the nanocomposite with 0.4 wt% of clay, which showed the highest crystallization rate. The Avrami equation was able to describe the isothermal crystallization of the neat PCL and PCL/clay nanocomposite up to a critical value of the relative crystallinity, were deviation from the model was observed. This critical value was reduced by the presence of nanoclay. The heating thermograms, performed on PCL and PCL/clay after isothermal crystallization showed a reduction of the melting temperature with the increase of the clay content, suggesting that the degree of perfection of the crystals and the degree of crystallinity achieved were affected by the restricted mobility of the chains, which did not allowed the growth of well developed lamellar crystals. Rheological measurements confirm the effect of clay on the crystallization kinetics observed with thermal analysis, with similar crystallization time scales. G' and G'' evolution during crystallization allowed a deeper insight into the crystallization phenomenon of the nanocomposites both at early stage and at the end of crystallization, leading to a new interpretation of the effect of intercalated and exfoliated phases on the viscoelastic properties of clay nanocomposites. The measurement of the viscoelastic properties of the molten or solidified nanocomposites gave information on the degree of exfoliation of this type of hybrid materials.

References

[1] Hambir S, Bulakh N, Kodgire P, Kalaonkar R, Jog JP. J Appl Polym Sci 2001;39:446.
[2] Galgali G, Ramesh C, Lele A. Macromolecules 2001;34:852.
[3] Rong MZ, Zhang MQ, Zheng YX, Zeng HM, Walter R, Friedrich K. Polymer 2001;42:167.
[4] Wang KH, Choi MH, Koo CM, Choi YS, Chung IJ. Polymer 2001;42: 9819.
[5] Okamoto M, Morita S, Taguchi H, Kim Y, Kotaka T, Tateyama H. Polymer 2000;41:3887.
[6] Yoon JT, Jo WH, Lee MS, Ko MB. Polymer 2001;42:329.
[7] Liu X, Wu Q. Polymer 2001;42:10013.
[8] Wang KH, Choi MH, Koo CM, Choi YS, Chung IJ. Polymer 2001;42: 9819.
[9] Lincoln DM, Vaia RA, Wang ZG, Hsiao BS. Polymer 2001;42:1621.
[10] Fornes TD, Yoon PJ, Keskkula H, Paul DR. Polymer 2001;42:9929.
[11] Gopakumar TG, Lee JA, Kontopoulou M, Parent JS. Polymer 2002; 43:5483.
[12] Liu X, Wu Q. Eur Polym J 2002;38:1383.
[13] Liu X, Wu Q, Berglund LA. Polymer 2002;43:4967.
[14] Wu Z, Chixin Z, Zhu N. Polym Testing 2002;21:479.
[15] Li J, Zhou C, Gang W. Polym Testing 2003;22:217.
[16] Tseng C-R, Wu J-Y, Lee H-Y, Chang F-C. Polymer 2001;42:10063.
[17] Fornes TD, Paul DR. Polymer 2003;44:3945.
[18] Kim SH, Ahn SH, Hirai T. Polymer 2003;44:5625.
[19] Nam JY, Ray SS, Okamoto M. Macromolecules 2003;36:7126.
[20] Lee JH, Park TG, Park HS, Lee DS, Lee YK, Yoon SC, Nam J-D. Biomaterials 2003;24:2773.
[21] Lepoittevin B, Devalckenaere M, Pantoustier N, Alexandre M, Kubies D, Calberg C, Jérôme R, Dubois P. Polymer 2002;43:4017.
[22] Hao J, Yuan M, Deng X. J Appl Polym Sci 2002;86:676.
[23] Jimenez G, Ogata N, Kawai H, Ogihara T. J Appl Polym Sci 1997;64: 2211.
[24] Winter HH, Mours M. Adv Polym Sci 1997;134:165.
[25] Di Y, Iannace S, Di Maio E, Nicolais L. J Polym Sci, Part B: Polym Phys 2003;41:670.
[26] Advani M. J Chem Phys 1940;8:212.
[27] Iannace S, Nicolais L. J Appl Polym Sci 1997;64:911.
[28] Zhang G, Yan D. J Appl Polym Sci 2003;88:2181.
[29] Inoue M. J Polym Sci Pt A 1963;1:2013.
[30] Wunderlich B. Macromolecular physics, vol. 2. New York: Academic Press; 1973.
[31] Gurato G, Gaidano D, Zannetti R. Makromol Chem 1978;179:231.
[32] Mudra I, Balazs G. J Therm Anal Calorim 1998;52:355.
[33] Khanna YP. Macromolecules 1993;26:3639.
[34] Lin YG, Mallin DT, Chien JCW, Winter HH. Macromolecules 1991; 24:850.